Supporting Information

Peeling and mesoscale dissociation of silk fibers for hybridization of electro-thermic fibrous composites

Lili Lv,[1,3] Xiangsheng Han,[1,3] Xiaochen Wu[1,2,] and Chaoxu Li[1,3,*]*

[1]Group of Biomimetic Smart Materials, Qingdao Institute of Bioenergy and Bioprocess Technology, Chinese Academy of Sciences, Songling Road 189, Qingdao 266101, P. R. China

[2]Department of Pharmacy, College of Chemical Engineering, Qingdao University of Science and Technology, Qingdao 266042, China

[3]Center of Material and Optoelectronics Engineering, University of Chinese Academy of Sciences, 19A Yuquan Road, Beijing 100049, P.R. China

Corresponding Authors:

(X. Wu) wuxc@qibebt.ac.cn

(C. Li) licx@qibebt.ac.cn

With 14 Pages, 20 Figures, and 1 Table in the Supporting Information.

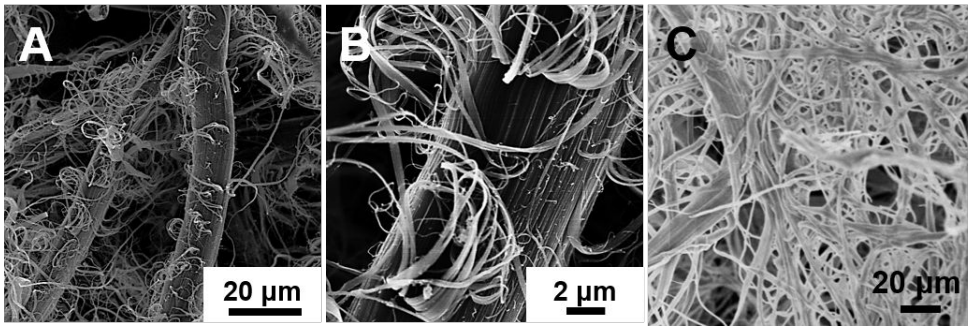

Figure S1. SEM images of silk fibers incubated in 8.8 M of urea for (A-B) 5 days and (C) 30 days at room temperature.

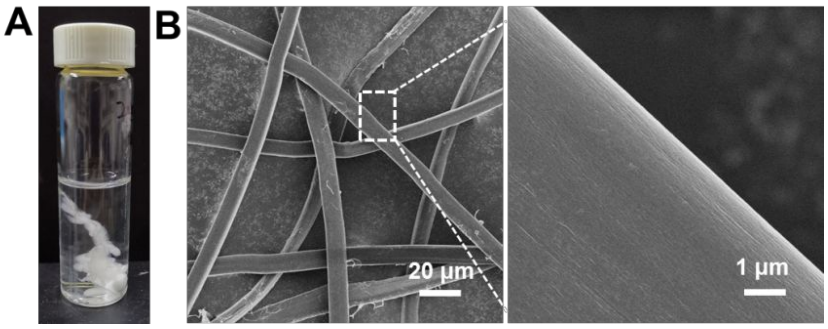

Figure S2. (A) Optical and (B) SEM images of silk fiber after incubating in H_2O at 25 ºC for 14 days.

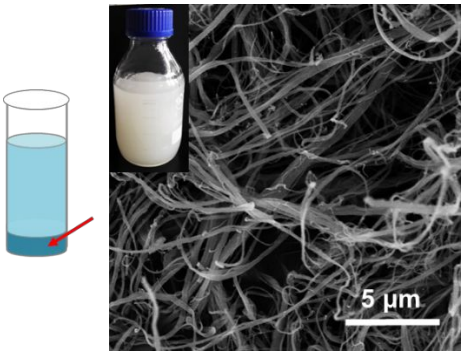

Figure S3. SEM image of un-dissociated microfibrils. Preparation procedure: 1 g of degummed silk incubated in 500 g of urea (8.8 M) for 30 days at room temperature, followed by ultra-sonication at 300 W for 180 s, and centrifugation at 4000 rpm for 10 min to get the sediment.

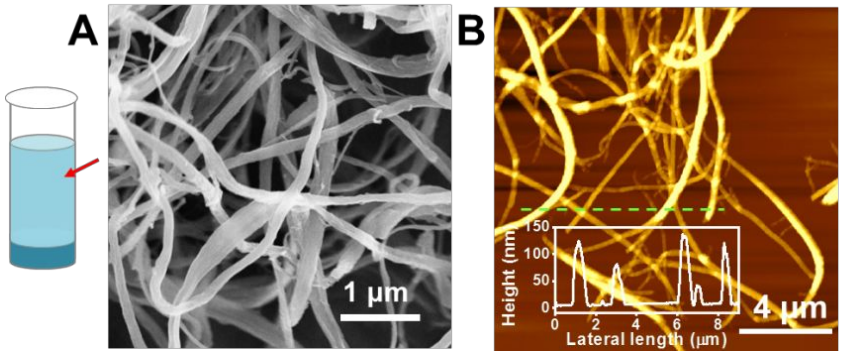

Figure S4. (A) SEM image and (B) Tapping mode AFM image with height profile of silk microfibrils. Preparation procedure: 1 g of degummed silk incubated in 500 g of urea (8.8 M) for 30 days at room temperature, followed by ultra-sonication at 300 W for 180 s, and centrifugation at 4000 rpm for 10 min to get the supernatant.

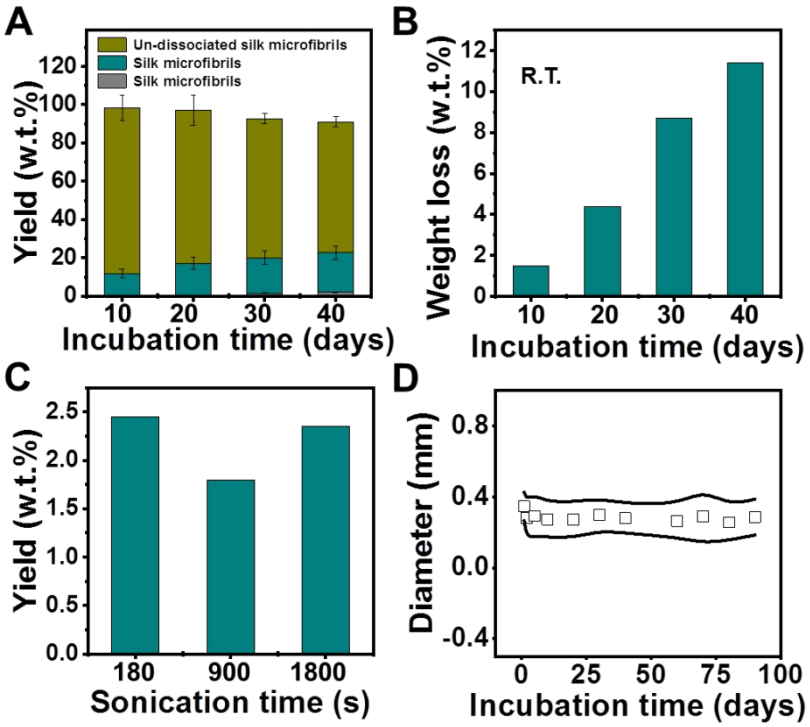

Figure S5. (A) Yields of un-dissociated microfibrils, microfibrils, and nanofibrils obtained at various incubation days. Preparation procedure: 1 g of degummed silk incubated in 500 g, 8.8 M of urea at room temperature. (B) Total weight loss of silk fiber calculated from (A). (C) Effect of ultrasonic time on the yield of nanofibrils. 1 g of degummed silk was incubated in 500 g of urea (8.8 M) at room temperature for 30 days, sonication for various time and centrifugation at 9000 rpm to get the nanofibrils. (D) Diameter distributions of silk microfibrils acquired at different incubation time. Preparation procedure: 1 g of degummed silk incubated in 500 g, 8.8 M of urea at room temperature, followed by ultra-sonication at 300 W for 180 s, and centrifugation at 4000 rpm for 10 min to get the supernatant.

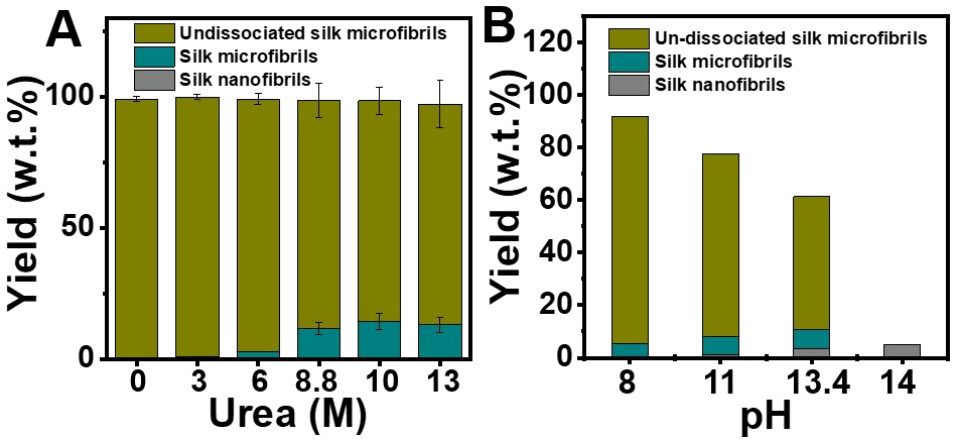

Figure S6. (A) Yield dependence of microfibrils and nanofibrils on the concentration of urea at 25 °C for 10 days. (B) Yield dependence of microfibrils and nanofibrils on pH at 25 °C for 4 days, with 8.8 M of urea.

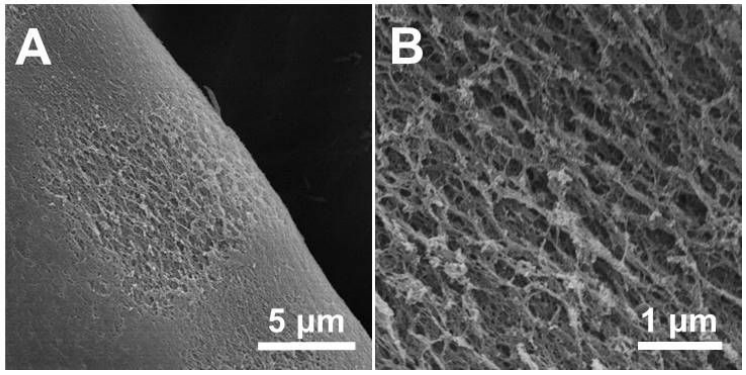

Figure S7. SEM images of silk fibers incubated in formic acid for 30 s at room temperature at different magnifications.

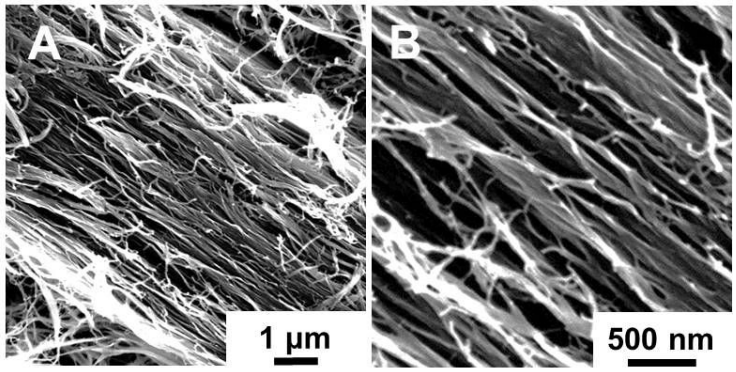

Figure S8. SEM images of silk fibers incubated with NaOH (5 w.t.%) for 24 h at room temperature at different magnifications.

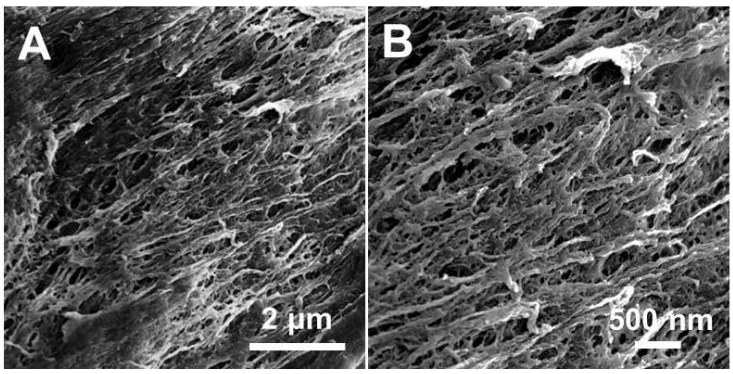

Figure S9. SEM images of silk fibers incubated in HFIP for 7 h at 80 °C at different magnifications.

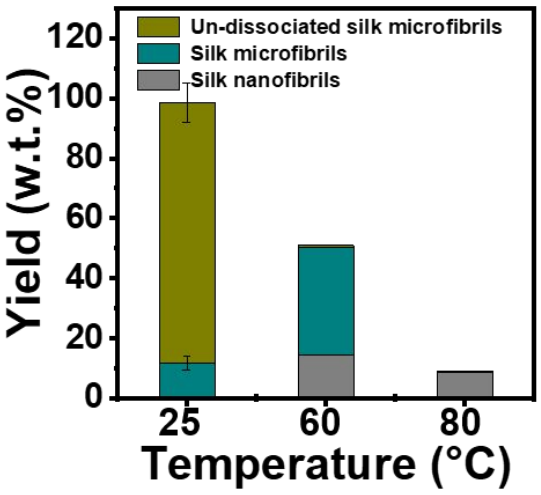

Figure S10. (A) Yield dependence of un-dissociated microfibrils, microfibrils and nanofibrils on incubation temperature. Urea concentration: 8.8 M, reaction time: 10 days.

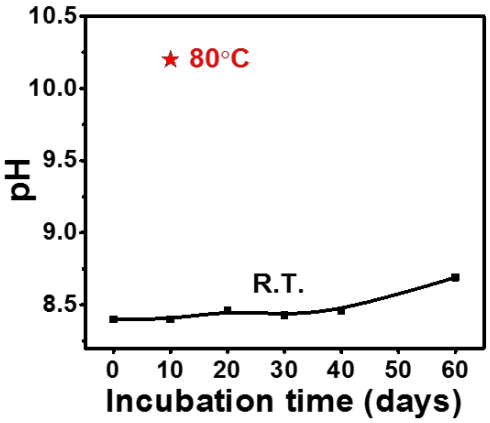

Figure S11. System pH variation of silk fibers incubated in urea (8.8 M) under different time and temperature.

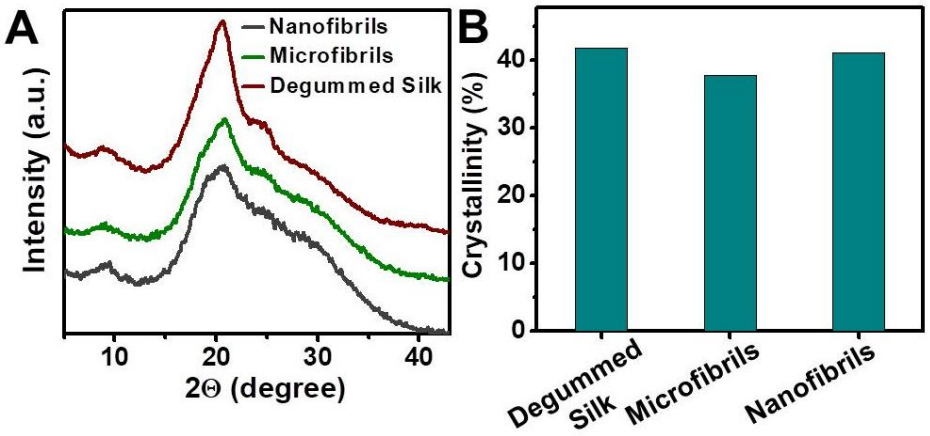

Figure S12. (A) XRD patterns and (B) crystallinity of freeze-dried silk nanofibrils, microfibrils and degummed silk.

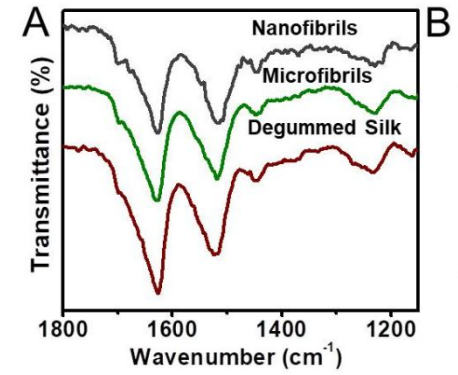

B

Band position (cm^{-1})	Assignment
1620-1635	Native β-sheet
1640-1660	Random coil and α-helix
1665-1685	β-turn
1690-1705	Antiparallel amyloid β-sheet

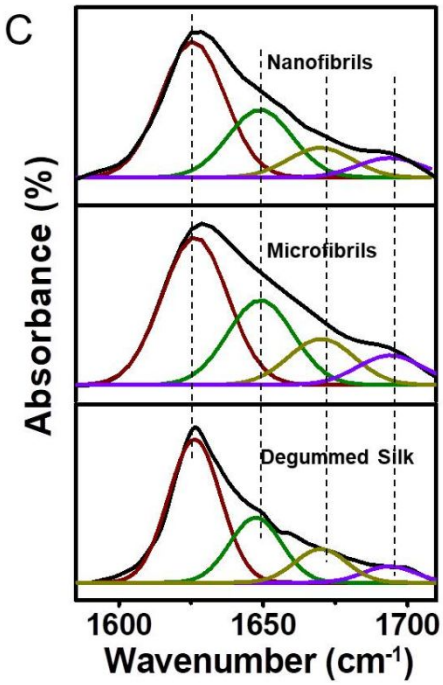

Fig. S13 (A) FTIR spectra, (B) standard of assignment amide I and (C) secondary structures of amide I bands of silk nanofibrils, microfibrils and degummed silk.

Fourier deconvolution of the infrared spectra covering the amide I region (1585-1710 cm^{-1}) was performed by the software Peak Fit.[1,2] The first derivative was applied to the original spectra in the amide I region, with 1% of Savitsky-Golay smoothing filter. Gaussian line shape profiles were used in the fit process. The curve fitting was proceeded automatically with the software: (1) the initial band positions were fixed (1626 cm^{-1} for native β-sheet, 1650 cm^{-1} for random coil and α-helix, 1672 cm^{-1} for

β-turn, and 1695 cm^{-1} for antiparallel amyloid β-sheet), and the band widths and heights were unconstrained. (2) The program was initiated to adjust the band widths and heights automatically to produce a reconstituted spectrum that matched the original deconvoluted one. (3) The deconvoluted amide I spectra were area-normalized where the relative area of the single band was used to determine the fraction of the secondary structural contents.

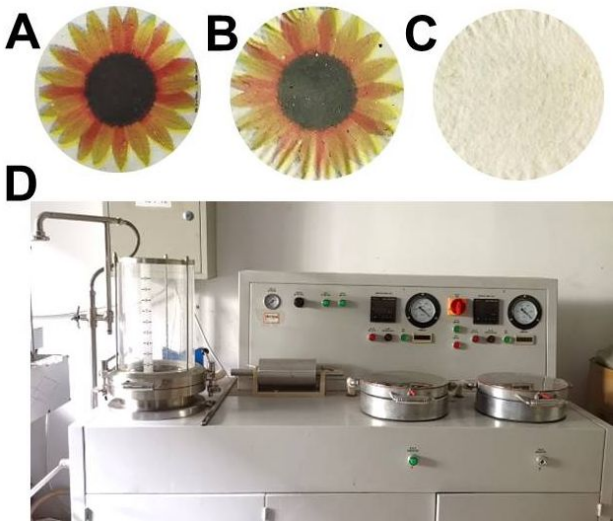

Figure S14. (A-C) Optical images of films of silk nanofibrils (A), microfibrils (B) and un-dissociated microfibrils (C) produced *via* filtration and air-drying at 60 °C. (D) Papermaking machine.

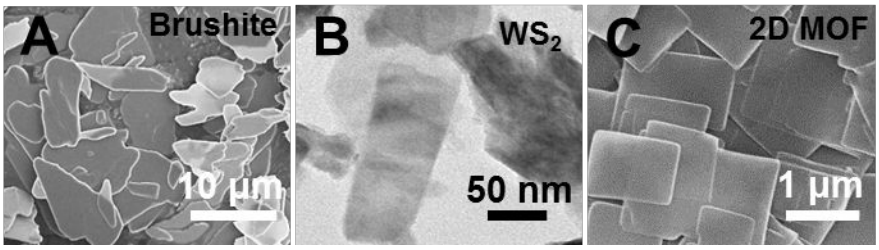

Figure S15. (A) SEM image of brushite nanoplatelets, (B) TEM image of WS_2 nanosheets, and (C) SEM image of CuBDC.

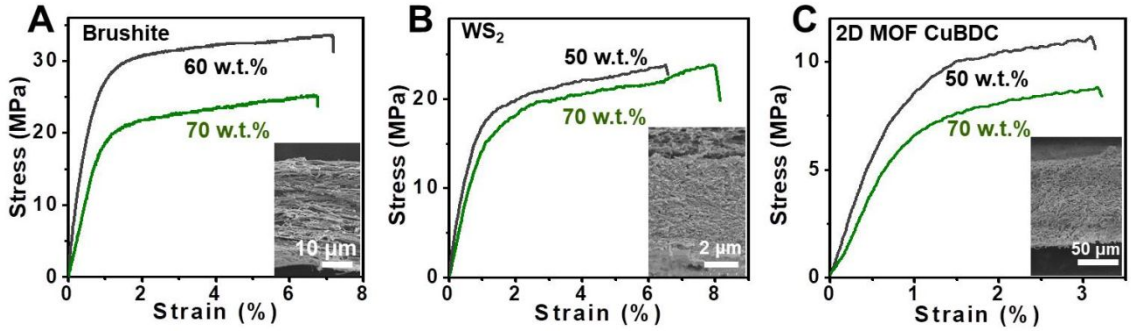

Figure S16. Typical stress-strain curves of composites of silk microfibrils with (A) brushite nanoplatelets (60-70 w.t.%), (B) WS_2 nanosheets (50-70 w.t.%) and (C) CuBDC (50-70 w.t.%). The corresponding cross-sectional SEM images of the composites were given as the inset.

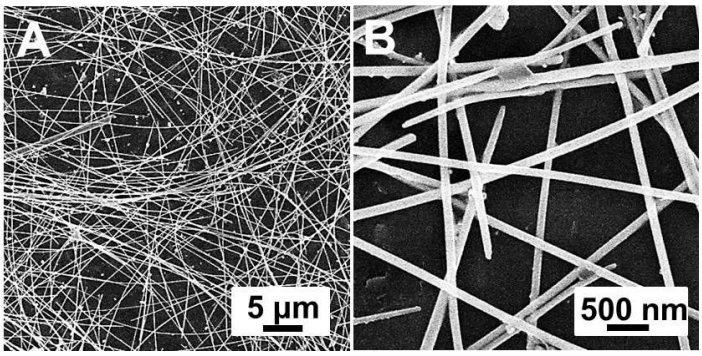

Figure S17. SEM images of Ag nanowires at different magnifications.

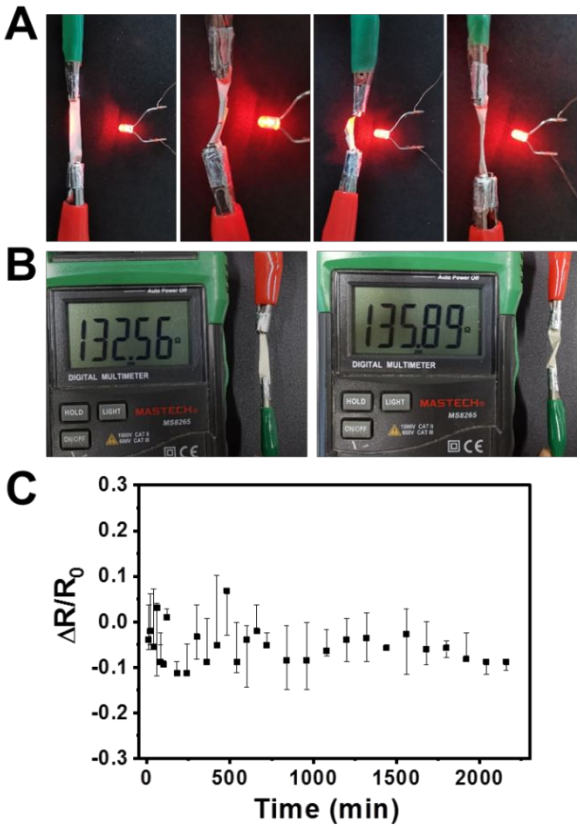

Figure S18. (A-B) Conductivity endurance of composite films of silk microfibrils and Ag nanowires against folding and twisting. (C) Conductivity endurance of composite film of silk microfibrils and Ag nanowires against rubbing. The conductive films were pasted on a glass slide with the two ends connected to a digital multimeter (MS8265, Mastech Ltd. Dongguan, China), then transferred onto a magnetic stirrer with a poly(tetrafluoroethylene) coated magnetic stir bar stirring at 60 rpm, and the resistance variations were recorded and plotted.

Figure S19. Composite film of silk microfibrils with Ag nanowires producing *via* liquid-casting: (A) Insulating silk-rich layer, and (B) conductive Ag-rich layer.

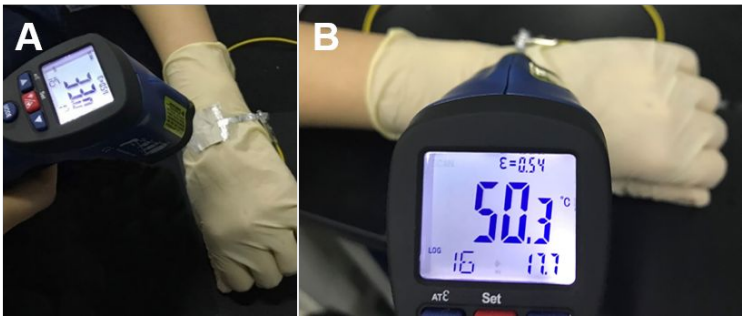

Figure S20. Composite film of silk microfibrils and Ag nanowires as thermotherapy pads with applied biases of (A) 0 V and (B) 3V. Sheet resistance: 25 Ω/sq.

Table S1. Mechanic analysis of films of silk nanofibrils, microfibrils, and un-dissociated microfibrils produced *via* filtration.

	Young's Modulus (GPa)	Strain (%)	Ultimate Stress (MPa)
Nanofibrils	1.7±0.5	7.3±3.7	40.7±3.5
Microfibrils	3.6±0.9	19.7±4.5	68.5±16.1
Un-dissociated	1.2±0.2	4.5±1.3	23.3±4.2

References:

(S1) Kong, J.; Yu, S., Fourier Transform Infrared Spectroscopic Analysis of Protein Secondary Structures. *Acta Bioch. Biophys. Sin.* **2007,** *39*, 549-559. DOI: 10.1111/j.1745-7270.2007.00320.x.

(S2) Hu, X.; Kaplan, D.; Cebe, P., Determining Beta-Sheet Crystallinity in Fibrous Proteins by Thermal Analysis and Infrared Spectroscopy. *Macromolecules* **2006***, 39*, 6161-6170. DOI: 10.1021/ma0610109.